

Article

Developmental Study of Soot-Oxidation Catalysts for Fireplaces: The Effect of Binder and Preparation Techniques on Catalyst Texture and Activity

Pauliina Nevalainen, Niko Kinnunen *  and Mika Suvanto

University of Eastern Finland, Department of Chemistry, P. O. Box 111, FI-80101, Joensuu, Finland;
Pauliina.Nevalainen@uef.fi (P.N.); mika.suvanto@uef.fi (M.S.)

* Correspondence: niko.kinnunen@uef.fi

Received: 8 October 2019; Accepted: 13 November 2019; Published: 15 November 2019



Abstract: An awareness of increasing climate and health problems has driven the development of new functional and affordable soot-oxidation catalysts for stationary sources, such as fireplaces. In this study, $\text{Al}(\text{OH})_3$, water glass and acidic aluminium phosphate binder materials were mixed with soot-oxidation catalysts. The effect of the binder on the performance of the $\text{Ag}/\text{La}-\text{Al}_2\text{O}_3$ catalyst was examined, while the $\text{Pt}/\text{La}-\text{Al}_2\text{O}_3$ catalyst bound with $\text{Al}(\text{OH})_3$ was used as a reference. Soot was oxidised above $340\text{ }^\circ\text{C}$ on the $\text{Ag}/\text{La}-\text{Al}_2\text{O}_3$ catalyst, but at $310\text{ }^\circ\text{C}$ with same catalyst bound with $\text{Al}(\text{OH})_3$. The addition of water glass decreased the catalytic performance because large silver crystals and agglomeration resulted in a blockage of the support material's pores. $\text{Pt}/\text{La}-\text{Al}_2\text{O}_3$ bound with $\text{Al}(\text{OH})_3$ was ineffective in a fireplace environment. We believe that AgO_x is the active form of silver in the catalyst. Hence, $\text{Ag}/\text{La}-\text{Al}_2\text{O}_3$ was shown to be compatible with the $\text{Al}(\text{OH})_3$ binder as an effective catalyst for fireplace soot oxidation.

Keywords: binder; silver; $\text{Al}(\text{OH})_3$; fireplace; soot emission

1. Introduction

Soot is a natural product that forms during incomplete combustion when organic compounds and fossil fuels are pyrolysed [1]. Due to a lack of oxygen, burning is often incomplete, especially in fireplaces, which leads to the formation of particulate matter (PM) and soot. In addition, polyaromatic hydrocarbons formed during the combustion process are linked to soot particles [2], and soot PM is harmful to health, with exposure increasing the risk of cardiovascular disease [1,3,4]

Wood is a main household heating source in Europe, especially in winter, with fireplace emissions approaching dangerously high levels [5,6]. In particular, domestic indoor air quality can suffer dramatically if wood is used as the heating source [7,8]. A standard and systematic emissions control system, such as those for vehicles, does not exist in Europe; however, the EU plans to restrict domestic fireplace and stove emissions, such as $\text{PM}_{2.5}$, in the near future [6]. PM emission standards for new fireplaces already exist in some states of the US, which creates more pressure for fireplace manufacturers in Europe to develop efficient working systems that reduce the formation of soot and particulate matter; however, technology for the prevention of soot formation in wood-combustion processes is still in its infancy.

Oxidation processes occur in the top layers of soot particles in which the carbon content is converted into CO and CO_2 , which simultaneously reduces soot mass [9]. Soot oxidises naturally at a sufficiently high temperature and oxygen level; however, these parameters are not well-controlled in a fireplace. Soot formation in diesel engines has been widely studied and is a well-known health risk; this problem has been solved using a catalyst that oxidises soot particles via the oxidation of NO to

NO₂. [10]. Noble metals, such as Pt, are normally effective in catalysts designed for use in vehicles and have been used in diesel vehicles to reduce soot accumulation in diesel particulate filters [11,12]. Pt is also used in fireplace soot-oxidation catalysts [13,14]; for instance Pt-, Pt/Pd- and Ce-supported materials have been studied as catalysts for the reduction of CO and volatile organic compounds (VOC) emissions in fireplaces [15–17]; however, Pt- and Pd-containing catalytic converters for residential wood combustion have been shown to increase the emissions of harmful chlorophenols, polychlorinated dibenzo-p-dioxins and polychlorinated dibenzofurans [18]. With this in mind, as well as the high costs of platinum-group metals, other solutions have been explored, with Ag, among non-platinum-group metal catalysts, exhibiting promising catalytic soot-oxidation performance in diesel vehicles [19–23]. In fact, according to previous studies, Ag has been shown to exhibit superior performance to Pt at oxidising soot in studies that tailor catalysts to fireplace conditions [24–26].

In systems designed for cars, the catalyst is attached to a honeycomb structure by dipping, painting or spraying it with ceramic- or metal-substrate materials. Special materials are used to bind the catalyst to the substrate surface to ensure that it remains attached and tolerates stress [27,28]. These binders increase the adhesion between the substrate and catalyst materials, and act as joining glues. In this study, we aimed to prepare fireplace soot-oxidation catalysts in which the binder is added to the catalyst during preparation. These painted catalyst substrates were placed in the smoke chambers of the fireplace at a temperature suitable for the catalyst to operate. We prepared a series of alumina-supported Ag materials and studied their performance during soot-oxidation catalysis. The effects of various binders, namely sodium silicate (water glass), acidic aluminium phosphate and aluminium hydroxide, on the performance of the catalyst were investigated. In addition, a Pt catalyst bound with Al(OH)₃ was prepared as a reference. Al(OH)₃ has been used as a binder in CaO-based pellets that capture CO₂ [29]; Al(OH)₃ has often been used as a precursor for aluminium phosphate binders, and water glass is versatile since the adhesive and binding properties of sodium silicate have been used to prepare thermally resistant ceramic paints and casting moulds [30,31]. Aluminium phosphate has also been used as a binding and coating material in the ceramics industry [32,33]. Both water glass and acidic aluminium phosphate transform into ceramics upon heating; however, more deformations are observed with water glass as the binder during severe heating [34]; we assume that the addition of the binder alters the catalyst's structure and its chemical composition, thereby influencing its catalytic performance.

2. Results and Discussion

2.1. The Effect of the Binder on the Textural Properties of the Catalyst

Studying the textural properties of the catalyst, including the dispersion of the active metal and the Brunauer–Emmett–Teller (BET) surface area, is important because catalytic reactions occur on the surfaces of catalysts. In theory, more collisions occur on the surface with increasing surface area; consequently, knowing the surface area of the catalyst provides more detail about the operation of the catalyst and its activity [35,36]. However, catalyst activity cannot be straightforwardly assumed to increase with increasing surface area [37]. How the active metal species are dispersed also provides insight into how the catalyst operates because a catalyst with highly dispersed active-metal species contain many active sites on its surface [38]. Figure 1 shows the relationship between the BET surface area of each catalyst in this study and the degree of dispersion of its active metal. Catalysts that contained water glass, namely Ag-WG2 and Ag-WG3, exhibited the lowest BET surface areas and levels of active-metal dispersion. In addition, Ag-WG1 suffered from low dispersiveness, despite having a higher surface area. On the other hand, insignificant differences in the BET area and active-metal dispersiveness were observed when the Al(OH)₃ binder was used, as in catalysts Ag-AH1 and Ag-AH3. The lower BET surface areas of the water-glass-containing catalysts were the consequence of the preparation method and the mixing order, which differed between Ag-WG2 and Ag-WG3, and Ag-WG1, which exhibited a similar BET area to that of Ag-AH1. In particular, when the water glass binder was

first mixed with the support material followed by the addition of Ag, as in the case of Ag-WG3, the water glass is presumed to have blocked the pores of the support material, resulting in limited access to the silver inside the pores, as highlighted by the low BET surface area of this catalyst. These results indicate that the preparation method was very important when water glass was used as the binder. Reference Pt/La-Al₂O₃, namely R3, exhibited the highest BET surface area and degree of active-metal dispersion (Figure 1); Pt was clearly better dispersed than Ag in these catalysts.

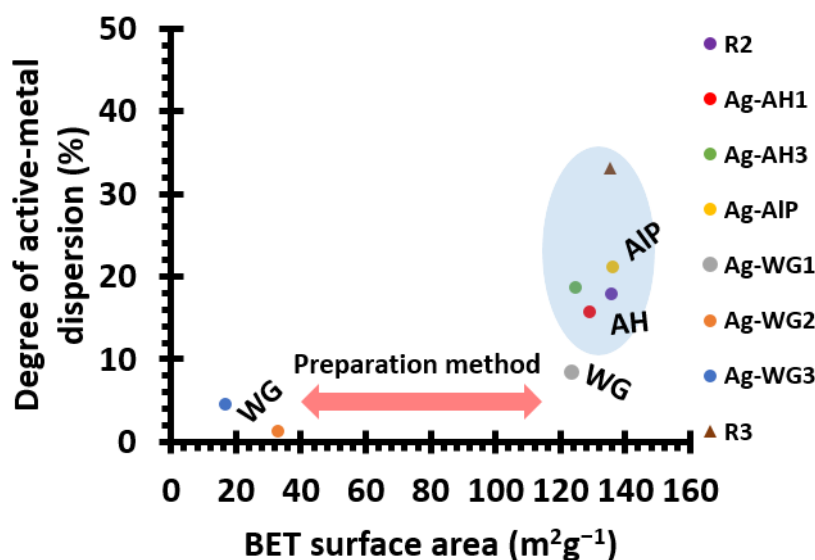


Figure 1. Showing the relationship between the degree of active-metal dispersion and the BET surface area of the catalyst. The blue area highlights the most promising catalysts according to the BET surface area versus dispersion results. For more details about the catalyst, see Table 1.

Table 1. Ag and Pt catalysts prepared in this study: binder materials, BET surface areas and levels of active-metal dispersion.

Catalyst	Support Material	Active Metal	Binder Material	BET Surface Area (m ² g ⁻¹)	Active-Metal Dispersion (%)
R1	La-Al ₂ O ₃	-	-	157.1	-
R2	La-Al ₂ O ₃	Ag	-	135.6	17.9
Ag-AH1	La-Al ₂ O ₃	Ag	Al(OH) ₃	129.0	15.8
Ag-AH3 ^a	La-Al ₂ O ₃	Ag	Al(OH) ₃	124.8	18.7
Ag-AIP	La-Al ₂ O ₃	Ag	Acid aluminium phosphate	136.2	21.2
Ag-WG1	La-Al ₂ O ₃	Ag	Water glass	123.6	8.4
Ag-WG2 ^b	La-Al ₂ O ₃	Ag	Water glass	32.7	1.3
Ag-WG3 ^a	La-Al ₂ O ₃	Ag	Water glass	16.7	4.5
R3	La-Al ₂ O ₃	Pt	Al(OH) ₃	135.4	33.1

^a Preparation order: (I) support material + binder (calcined at 500 °C for 3 h), then (II) active metal (calcined at 500 °C for 3 h). ^b Preparation order: (I) binder + active metal, then (II) support material.

Figure 2 shows SEM images of the catalysts prepared in this study before grinding and coating. Note that the size and shape of the catalyst particle may vary in the coated catalyst because of grinding of the catalyst coating before its deposition onto the substrate. Silver particles could be observed in the SEM images when a high accelerator voltage was used; Ag appears in these SEM images as bright crystalline particles. Figure 2c,d shows agglomerated Ag on the support material when water glass was used as the binder. These SEM images revealed that the Ag particles were larger in Ag-WG1 and Ag-WG3 than in any other catalyst. Figure 2b,e,f verifies that the corresponding catalysts were well-dispersed (Table 1). The addition of Al(OH)₃ or the acidic aluminium phosphate binder to the catalyst did not substantially decrease its BET surface area or degree of active-metal dispersion.

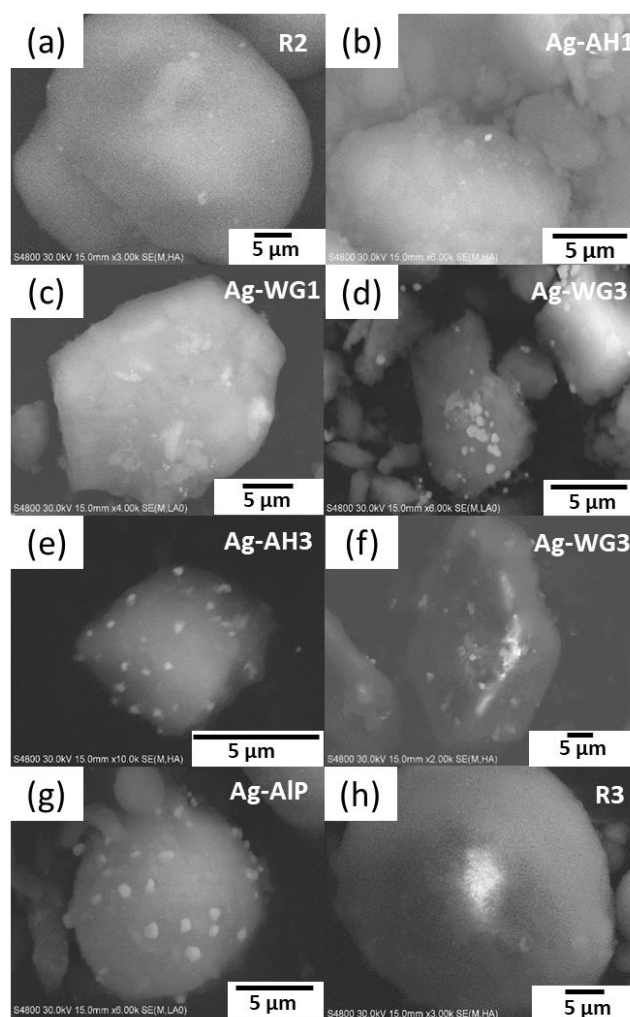


Figure 2. SEM images of catalysts prepared in this study: (a) R2, (b) Ag-AH1, (c) Ag-WG1, (d) Ag-WG3, (e) Ag-AH3, (f) Ag-WG2, (g) Ag-AIP and (h) R3. Scale bars: 5 μm . For more details about the catalysts, see Table 1.

2.2. Soot-Oxidation Activities of the Catalysts

2.2.1. Effect of the Binder on Activity

The soot-oxidation results for the various catalysts are displayed in Figure 3a. Carbon was converted into CO and CO₂ during soot oxidation. FTIR detected the CO₂ and CO formed in the emissions, and the catalysts' performance was evaluated on the basis of the soot-oxidation temperature of each catalyst; the lower the soot-oxidation temperature, the better the catalytic performance. To compare soot-oxidation temperatures from different experiments, we considered the highest CO₂ concentration; however, despite the concentration of soot in the sample affecting the amount of converted CO₂, it did not affect the soot-oxidation temperature. Sample R1, which was pure soot mixed with the La-alumina support material, exhibited an oxidation temperature of 475 °C, while the Ag-AH1 catalyst displayed the lowest soot-oxidation temperature of 310 °C; Ag-AH1 also formed insignificant amounts of CO (Figure 3b). The highest CO concentrations were produced by the water-glass-containing catalysts Ag-WG2 and Ag-WG3. If we compare the data for reference catalyst R2, which was the Ag/La-Al₂O₃, and Ag-AH1, it is clear that addition of the binder decreased the soot-oxidation temperature by 40 °C, whereas in the case of Ag-WG1, the addition of the water-glass binder increased the soot-oxidation temperature by almost 20 °C over that of Ag-AH1. The water-glass binder expanded during calcination and formed small crystallites; the expanding binder possibly

forced the Ag, which was already inside the pores of the support material, out of the pores during calcination. The soot-oxidation temperature of the Ag-AIP catalyst was between that of Ag-AH1 and Ag-WG1. The acidic aluminium phosphate binder was slightly superior to water glass in terms of catalytic performance, but it lost its $\text{Al}(\text{OH})_3$ binder. Irrespective of the catalyst processing method, the water-glass binder resulted in an inferior catalytic performance. Aided by the silver catalyst and the $\text{Al}(\text{OH})_3$ binder, the soot-oxidation temperature was lower by 165°C compared to that of soot oxidation in the absence of the catalyst. This can be explained, at least partially, by the addition of $\text{Al}(\text{OH})_3$ binder, which increased the active-metal dispersion (Figure 1 and Table 1), and thus may improve the contact between the catalyst and the soot. Gardini et al. [39] studied the commercial unsupported Ag nanopowder catalyst for soot oxidation. They suggested that Ag particles' mobility increases contact between the soot and the catalyst during the soot oxidation, thus improving its activity in the reaction. In our case, the catalysts were La-alumina-supported and Ag particles' mobility could be more restricted than in the case of a Ag nanopowder, even though it is plausible that $\text{Al}(\text{OH})_3$ binder could influence the Ag mobility and thus improve the contact between the soot and the catalyst. In addition, $\text{Al}(\text{OH})_3$ has also been shown to improve alumina porosity; hence, its phenomenal dispersing ability in the matrices in this study can be explained in terms of the same particle size distribution and residual charge density [40]. Clearly, $\text{Al}(\text{OH})_3$ improved the performance of the Ag/La- Al_2O_3 catalyst.

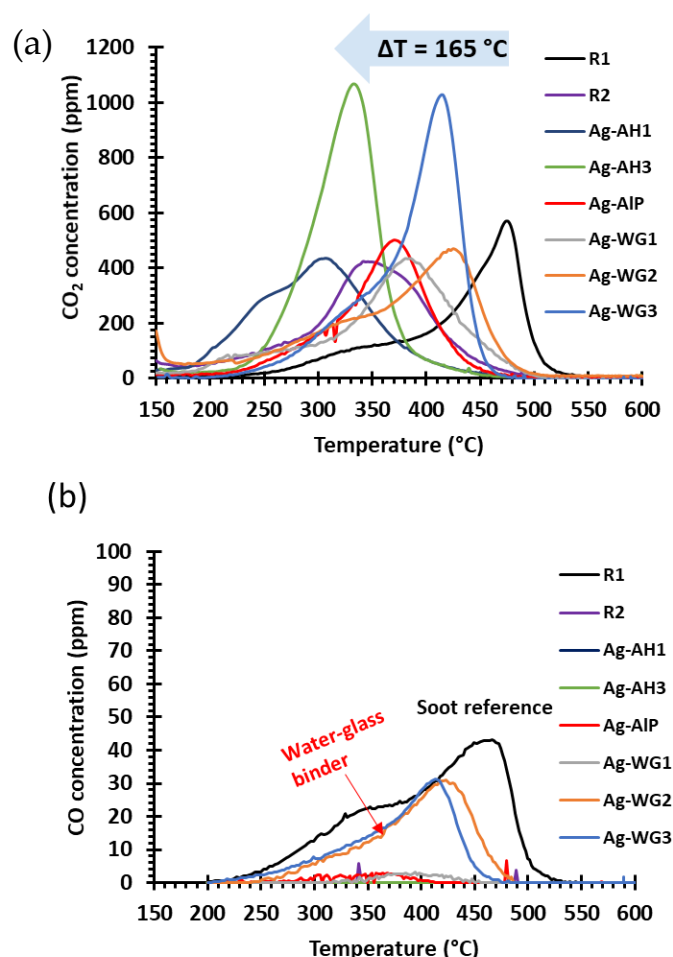


Figure 3. (a) Soot-oxidation performance and (b) CO formation for the silver catalysts and the soot reference. The difference in the soot-oxidation temperatures of samples R1 and Ag-AH1 was 165°C . For more details about the catalysts, see Table 1.

2.2.2. Steady-State Soot-Oxidation Activity

The temperature in a fireplace chimney during wood burning may not necessarily exceed 370 °C; hence, it is important to examine the steady-state performance of the catalyst. The carbon content of the soot produced by the Ag-AH1 catalyst was subjected to microanalysis before and after the catalyst–soot mixture was heated to 330, 350 and 370 °C for 30 min, and then quickly cooled. Table 2 shows that almost the entire carbon content of the soot was converted to gaseous CO₂. Soot is a very-light fine powder, which makes soot handling and weighing challenging. As a consequence, the calculated initial carbon contents differ slightly from those measured.

Table 2. Carbon content before and after soot oxidation at 330, 350 and 370 °C for 30 min.

Temperature (°C)	Initial Carbon Content (%)	Carbon Content After Heating (%)
330	3.91	0.18
350	4.49	0.15
370	4.26	0.15

The calculated value of the initial carbon content was 4.76%, which was calculated based on the soot carbon content and the amount of soot in the sample.

2.2.3. Comparing the Ag and Pt Soot-Oxidation Catalysts

Figure 4 displays the soot-oxidation performance of Ag- and Pt-containing catalysts, namely Ag-AH1 and the reference La-Al₂O₃ R3, respectively. Both catalysts contained the same molar amounts of metal, so their performance could be directly compared. The ability of silver to oxidise soot was notably superior to that of Pt; R3 oxidised soot slowly, with the highest CO₂-emission peak observed close to 500 °C. The poor performance of the Pt catalyst was possibly ascribable to the added Al(OH)₃ binder; however, the SEM image (Figure 2h), BET surface area and level of active-metal dispersion (Table 1 and Figure 1) did not support this hypothesis. In diesel particulate filters, NO₂ oxidises soot, whereas in our study NO or NO₂ were not present during the measurements. It is likely that the oxidation of soot with the Pt catalyst required the assistance of NO; hence, Pt alone was unable to efficiently oxidise soot because the level of NO₂ generated under fireplace conditions was rather low [25,26]. Figure 5 shows the soot-oxidation temperature as a function of the dispersiveness of the active metals in the catalyst in this study. As is clear, the silver catalysts were superior to the platinum catalyst in terms of soot-oxidation activity, despite platinum being notably better dispersed in the catalyst than silver.

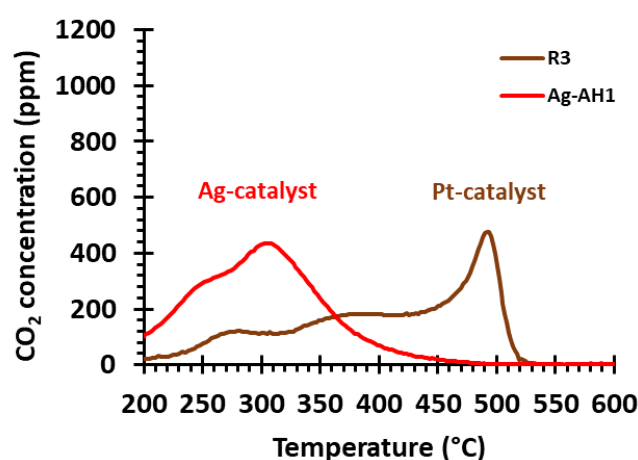


Figure 4. Performance of the Ag-AH1 and R3 catalysts. For more details about the catalysts, see Table 1.

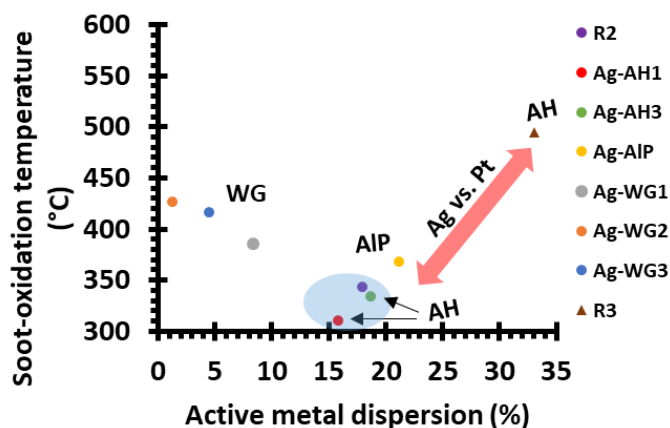


Figure 5. Relationship between the soot-oxidation temperature and the degree of active-metal dispersion. The blue area highlights the most promising catalysts. For more details about the catalysts, see Table 1.

2.3. Powder X-ray Diffraction Patterns of the Catalysts

Having a better understanding of the structure–activity relationship of the various catalysts, powder X-ray diffraction (PXRD) patterns were acquired, the results of which are displayed Figure 6. Metallic Ag peaks (Figure 6a) appeared at 2θ values of 38.0° , 44.5° , 64.5° , 77.5° and 81.5° in the patterns of all silver-containing catalysts. Catalyst R2, which contained the same amount of silver as the other catalysts, exhibited Ag peaks in its PXRD pattern that were very low in intensity, which was consistent with small crystals; in addition, based on the SEM image in Figure 2a and the dispersion data, we concluded that its silver particles were well-dispersed (Table 1) deep within the support material’s pores. The PXRD data revealed that the addition of the binder increased the Ag crystallinity remarkably, especially in the case of the water-glass binder. Ag-WG3 exhibited the most intense Ag peaks in its PXRD pattern, which supports the hypothesis that its Ag crystals were too large and were not well dispersed on the support material, as seen in its SEM image (Figure 2d); this clearly affected the catalytic performance. While we have assumed that catalytic performance decreases with increasing crystallinity, the highly crystalline Ag-AH3 exhibited a rather good soot-oxidation activity. Consequently, there may be other textural properties in addition to the BET surface area and dispersiveness that were responsible for the good soot-oxidation activities of some of the catalysts. Examination of the PXRD patterns of catalysts R2, Ag-AH1 and Ag-AH3 (Figure 6b) revealed additional peaks at 2θ values of 33° and 34° . We could disregard $\text{Al}(\text{OH})_3$ as being responsible for these peaks, since these peaks were present in the pattern of the binderless catalyst R2; these peaks most likely belonged to silver oxide. We believe that the presence of silver oxide enhanced the catalytic performance. Aneggi et al. demonstrated that the zero-oxidation state of silver is favoured on alumina as the support material and concluded that metallic silver is the most active form [22]. However, previous studies [25,41] have shown that AgO_x is the active form during the oxidation of soot; in our case, all the catalysts that contained AgO_x were the most active. Hence, we concluded that silver oxide was responsible for the good activities of catalysts R2, Ag-AH1 and Ag-AH3.

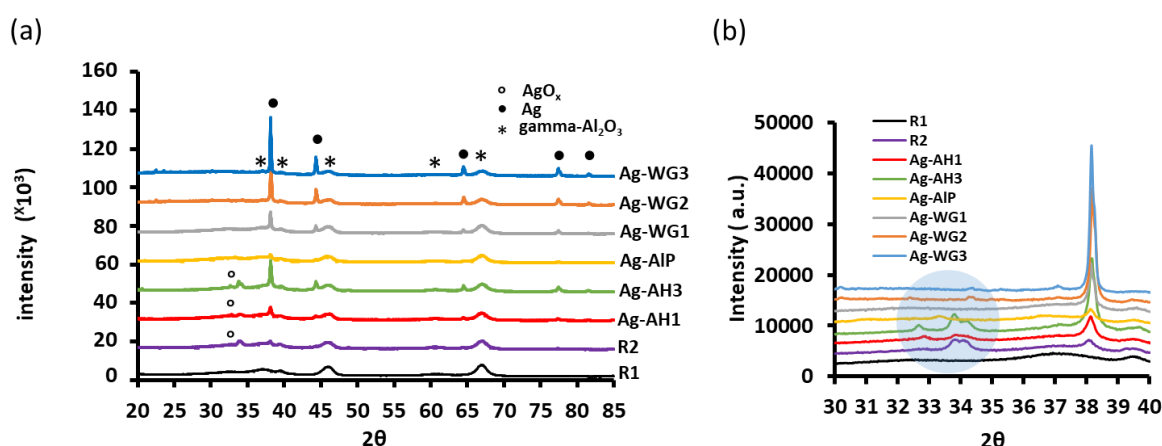


Figure 6. (a) Powder XRD patterns of the Ag-based catalysts in this study and the alumina reference. (b) Enlargement of the region in panel (a) where silver oxide peaks were observed, as highlighted by the blue circle. For more details about the catalysts, see Table 1.

3. Materials and Methods

Soot-oxidation catalysts and reference samples were prepared using a variety of mixing orders and preparation techniques, as detailed in Table 1. All catalysts were prepared using the wet-impregnation method on La-Al₂O₃ as the support material. The support material weight was 10 g and the active metal amount was calculated based on that. Water was added in the same ratio as the catalyst support material, 10 mL, such that the suspension was neither dry nor too wet. Catalysts were prepared in a beaker and mixed with a magnetic stirrer 2 h. Sample R1 contained only the support and was used as a reference material in the study. Catalyst R2, which consisted of active Ag metal on the La-Al₂O₃ support, was another reference. The following binders were selected for this study: aluminium hydroxide (Sigma-Aldrich, South Korea, reagent grade Al(OH)₃, solid); sodium silicate (also known as water glass, Sigma-Aldrich solution of Na₂SiO₃, reagent grade, liquid); and acidic aluminium phosphate (I), which was prepared by mixing 85% H₃PO₄ and Al(OH)₃ (Sigma-Aldrich, USA, reagent grade Al(OH)₃) at 150 °C for 2h, such that the P/Al ratio was 23 [34]. Silver nitrate (Alfa Aesar, Kandel, Germany, 99+% AgNO₃) was used as the active metal precursor and was first diluted with a small amount of deionised water before mixing with the other catalyst components. Except for reference sample R1 and catalyst R2, samples were prepared by adding the binder into aqueous solutions of catalysts; the Ag loading on the catalyst was 7 wt%. Binder concentrations were 5 wt% based on the dry weight of the support material. Catalysts Ag-AH1, Ag-WG1, Ag-AIP and R3 were prepared such that the support material and the aqueous active metal solutions were first mixed together, after which, the binder was added. Ag-WG2 was prepared by first mixing the binder and the active metal, followed by addition of the support material. After the mixing catalysts were dried in an evaporating dish in a fume cupboard for one day, all catalysts were finally calcined under oxidising conditions in a funnel oven at 500 °C for 3 h. R3 was the third reference catalyst and was prepared in the same manner as Ag-AH1, with platinum nitrate (Alfa Aesar 15 wt% Pt(NO₃)₄) instead of AgNO₃, such that the molar amounts of active metal were the same in both catalysts. Different preparation techniques were used for catalysts Ag-AH3 and Ag-WG3: the support material and the binder were mixed together, after which, the mixture was dried in an oven at 500 °C for 3 h. The dried mixture was then added to deionised water and diluted aqueous silver nitrate was added into the mixture. Finally, these two-step catalyst mixtures were calcined at 500 °C for 3 h.

The soot used in this study was collected from the chimney of a real domestic wood-burning fireplace. The carbon content of the soot was determined using elemental analysis (vario Micro cube elemental analyser, Elementar, Langensfeld, Germany) and was found to be ≈78%; the remaining residues were inorganic materials. In addition, the soot texture was characterised using Raman

spectroscopy (Figure 7) using a Renishaw inVia Raman Microscope (Renishaw, Gloucestershire, United Kingdom) with an Ar-ion laser at 514 nm. Three characteristic Raman peaks were observed for soot, namely the D-peak at 1370 cm^{-1} , the G-peak at 1600 cm^{-1} and a strong broad peak in the $2500\text{--}2800\text{ cm}^{-1}$ region that is common to all sp^2 materials. The first peak corresponds to distortions of the sp^2 crystal structure, while the latter corresponds to the stretching of C–C bonds in graphitic materials and it is common to sp^2 materials. The soot used in this study was related to the industrial and commercial soot that was studied by Sadezky et al. [42].

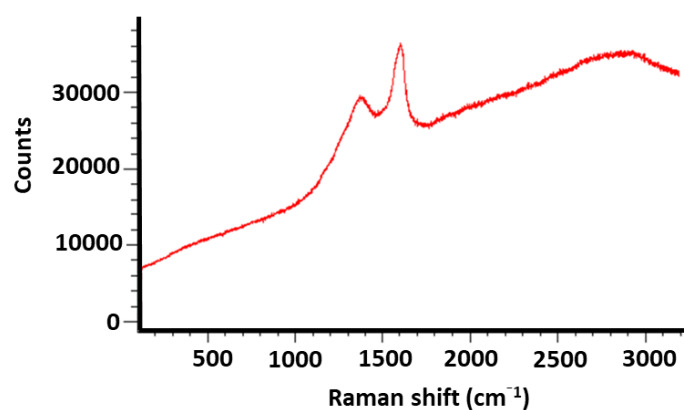


Figure 7. Raman spectrum of soot.

The catalyst surface areas were measured with a Quantachrome Autosorb-iQ gas-sorption analyser (Quantachrome Instruments, Boynton Beach, Florida) using 150-mg samples. All samples were degassed under vacuum at $350\text{ }^{\circ}\text{C}$ for 150 min prior to any experiment to remove moisture and residual air. These experiments were carried out at liquid nitrogen temperature ($-196\text{ }^{\circ}\text{C}$) and the surface areas were calculated according to Brunauer–Emmett–Teller theory.

The active-metal dispersions of Ag and Pt were examined as described above. All catalysts were reduced in 10% H_2/Ar for 1 h. Catalyst R3 was reduced at $500\text{ }^{\circ}\text{C}$, whereas the silver catalysts were reduced at $280\text{ }^{\circ}\text{C}$. The reducing temperatures were determined from temperature-programmed reduction (TPR) data; the Pt dispersion in catalyst R3 was determined using CO pulse titration at room temperature, assuming that the CO-to-surface-Pt ratio was 1:1 [43]. Silver dispersions were determined using the O_2 pulse titration method, assuming that the O_2 -to-surface-Ag ratio was 1:2 [44]; the oxygen was pulse-injected onto the catalyst at $100\text{ }^{\circ}\text{C}$.

The effects of binders and active metals on catalyst texture were studied using field-emission scanning electron microscopy (FE-SEM, Hitachi S-4800, Japan), at a working distance of 15 mm and an accelerator voltage of 30 kV. Powder X-ray diffraction (PXRD) experiments were conducted using a Bruker AXD D8 Advance diffractometer (Bruker, Karlsruhe, Germany), with a $\text{Cu K}\alpha$ radiation source. Diffraction patterns were collected in the $20\text{--}85^{\circ}$ 2θ range at a scan rate of $0.03^{\circ}/\text{min}$. Plastic and Si-mirror sample holders were used in these experiments.

Catalytic performance was determined using combustion experiments. Figure 8 shows a schematic picture of the combustion test rig. In a real fireplace, soot is solid, but is entrained by gaseous flow and collides with catalyst particles. In our experiment, soot was placed on the catalyst surface in the solid phase. Catalysts were in tight contact with the soot due to vibration-mill mixing. Tight contact has been shown to be the best way of mixing the catalyst and the soot in soot-oxidation processes [45]. The carbon content of the soot was considered when the soot and the catalysts were mixed together. The catalyst (400 mg) and soot (26 mg) were mixed via ball milling in two parts. La-alumina (200 mg) was then added with a spatula into 150 mg of the catalyst–soot mixture to decrease any possible temperature gradient. The mixture was divided into three separate layers in the reactor with quartz wool to minimise backup pressure. The catalyst samples (catalyst + glass wool) were placed inside the reactor tube in $\approx 2\text{ cm}$ increments starting from around 18 cm from the top, where the reactor tube inside

diameter was 1 cm and the length was 43 cm. The reactor was attached to a gas line heated with a programmed furnace with a heating rate of $7\text{ }^{\circ}\text{C}/\text{min}$. Soot oxidation was carried out using a 10% H_2O , 10% O_2 gas mixture (balanced with N_2), with a total gas flow rate of 1180 mL min^{-1} . Measurement was at normal pressure all the time. Water was added to the heated gas line with a syringe pump after the oven reached $110\text{ }^{\circ}\text{C}$ and the water was vaporised before it reached the catalyst. The water amount was monitored using FTIR spectroscopy (Gasetm FTIR DX-4000 spectrometer, Gasetm technologies, Helsinki, Finland). Gas mass-flow controllers were used to control the composition of the gas mixture. A thermocouple was placed right above the catalyst. The catalyst–soot mixture was finally heated from room temperature to $600\text{ }^{\circ}\text{C}$; oxidation products, mainly CO_2 and CO , were analysed with an online Gasetm FTIR DX-4000 spectrometer.

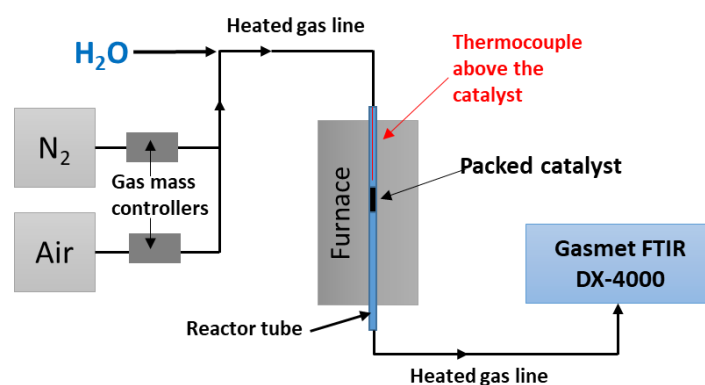


Figure 8. Schematic picture of combustion laboratory test rig.

4. Conclusions

In this study, three different binder materials, namely aluminium hydroxide, water glass and acidic aluminium phosphate, were added during the preparation of Ag fireplace soot-oxidation catalysts, and the effect of the binder on catalyst performance was studied. A Pt catalyst prepared with the $\text{Al}(\text{OH})_3$ binder was used as a reference. In addition, the effect of the preparation method on catalyst performance was also examined. Continuous-flow FTIR was used to study the effect of the binder on the soot-oxidation performance of each catalyst, while textural properties were determined using BET surface area analysis, the dispersiveness of the active metal, SEM and PXRD. The $\text{Ag}/\text{La}-\text{Al}_2\text{O}_3$ catalyst with the $\text{Al}(\text{OH})_3$ binder exhibited the best performance in terms of soot oxidation, and the performance of the $\text{Ag}/\text{La}-\text{Al}_2\text{O}_3$ catalyst improved notably after addition of the binder. Based on the PXRD data, silver was present in both metallic and oxidised forms when the $\text{Al}(\text{OH})_3$ binder was used, including the Ag and $\text{Ag}/\text{La}-\text{Al}_2\text{O}_3$ catalysts, which explained the superior performance of those catalysts. $\text{Al}(\text{OH})_3$ was also shown to improve the porosity of alumina, which makes it an excellent choice for use with the $\text{Ag}/\text{La}-\text{Al}_2\text{O}_3$ catalyst. The water-glass binder dramatically decreased the performance of the $\text{Ag}/\text{La}-\text{Al}_2\text{O}_3$ catalyst; very-low levels of dispersion, high Ag crystallinity and blockage of the support material pores by water glass were observed using SEM, while the Ag particles agglomerated on the top of the support material decreased the performance of the catalyst. Acidic aluminium phosphate did not provide performance results as good as those with the $\text{Al}(\text{OH})_3$ binder, even though it facilitated the highest levels of dispersion and the best BET surface areas among the Ag-based catalysts, which was ascribable to the absence of oxidised silver. The Ag catalysts exhibited notably better performance under fireplace conditions compared to the Pt catalyst, which was ascribable to the ability of Ag to directly oxidise carbon, whereas Pt-catalysed oxidation proceeded through a NO_x -assisted route, and wood burning did not produce high amount of NO_x . Overall, $\text{Al}(\text{OH})_3$ was found to be a good binder for use with a fireplace soot-oxidation catalyst when alumina was the support material and silver was the active metal.

Author Contributions: Methodology, P.N. and N.K.; validation, P.N.; formal analysis, P.N.; investigation, P.N.; writing—original draft preparation, P.N.; visualisation, P.N.; writing—review and editing, P.N. and N.K.; supervision, N.K.; resources, M.S.; data curation, M.S.; project administration, M.S.

Funding: The Finnish Funding Agency for Technology and Innovation (Business Finland EVIM project) and the European Regional Development Fund are gratefully acknowledged for their financial support within the EVIM project. SCITECO is gratefully acknowledged for their financial support.

Conflicts of Interest: The authors declare no conflict of interest.

References

1. Puri, I.K. *Environmental Implications of Combustion Processes*, 2nd ed.; CRC Press Inc.: Boca Raton, FL, USA, 1993.
2. Richter, H.; Howard, J. Formation of polycyclic aromatic hydrocarbons and their growth to soot—A review of chemical reaction pathways. *Prog. Energy Combust. Sci.* **2000**, *26*, 565–608. [[CrossRef](#)]
3. Pope, C.A.; Dockery, D.W. Health Effects of Fine Particulate Air Pollution: Lines that Connect. *J. Air Waste Manage. Assoc.* **2006**, *56*, 709–742. [[CrossRef](#)] [[PubMed](#)]
4. Kocbach Bølling, A.; Pagels, J.; Yttri, K.; Barregard, L.; Sallsten, G.; Schwarze, P.E.; Boman, C. Health effects of residential wood smoke particles: The importance of combustion conditions and physicochemical particle properties. *Part. Fibre Toxicol.* **2009**, *6*, 29. [[CrossRef](#)]
5. European Environment Agency. *Air Quality in Europe—2017*; Report No 13/2017; European Environment Agency: Copenhagen, Denmark, 2017. [[CrossRef](#)]
6. Fuller, G.W.; Sciare, J.; Lutz, M.; Moukhtar, S.; Wagener, S. New Directions: Time to tackle urban wood burning? *Atmos. Environ.* **2013**, *68*, 295–296. [[CrossRef](#)]
7. Salthammer, T.; Schripp, T.; Wientzek, S.; Wensing, M. Impact of operating wood-burning fireplace ovens on indoor air quality. *Chemosphere* **2014**, *103*, 205–211. [[CrossRef](#)] [[PubMed](#)]
8. Semmens, E.O.; Noonan, C.W.; Allen, R.W.; Weiler, E.C.; Ward, T.J. Indoor particulate matter in rural, wood stove heated homes. *Environ. Res.* **2015**, *138*, 93–100. [[CrossRef](#)]
9. Omidvarborna, H.; Kumar, A.; Kim, D.-S. Recent studies on soot modeling for diesel combustion. *Renew. Sustain. Energy Rev.* **2015**, *48*, 635–647. [[CrossRef](#)]
10. Neeft, J.P.A.; Makkee, M.; Moulijn, J.A. Diesel particulate emission control. *Fuel Process. Technol.* **1996**, *47*, 1–69. [[CrossRef](#)]
11. Russell, A.; Epling, W.S. Diesel oxidation catalysts. *Catal. Rev. Sci. Eng.* **2011**, *53*, 337–423. [[CrossRef](#)]
12. Heck, R.; Farrauto, R.; Gulati, S. *Catalytic Air Pollution Control Commercial Technology*, 3rd ed.; A John Wiley & Sons Inc. Publication: Hoboken, NJ, USA, 2009; p. 257.
13. Heck, R.; Farrauto, R.; Gulati, S. *Catalytic Air Pollution Control Commercial Technology*, 3rd ed.; A John Wiley & Sons Inc. Publication: Hoboken, NJ, USA, 2009; p. 392.
14. Ferrandon, M.; Berg, M.; Björnbom, E. Thermal stability of metal-supported catalysts for reduction of cold-start emissions in a wood-fired domestic boiler. *Catal. Today* **1999**, *53*, 647–659. [[CrossRef](#)]
15. Pieber, S.M.; Kambolis, A.; Ferri, D.; Bhattu, D.; Bruns, E.A.; Elsener, M.; Kröcher, O.; Prevot, A.S.H.H.; Baltensperger, U.; Emily, A.; et al. Remediation and Control Technologies Mitigation of secondary organic aerosol formation of log wood burning emissions by catalytic removal of aromatic hydrocarbons. *Environ. Sci. Technol.* **2018**. [[CrossRef](#)] [[PubMed](#)]
16. Carnö, J.; Berg, M.; Järås, S. Catalytic abatement of emissions from small-scale combustion of wood: A comparison of the catalytic effect in model and real flue gases. *Fuel* **1996**, *75*, 959–965. [[CrossRef](#)]
17. Ozil, F.; Tschamber, V.; Haas, F.; Trouvé, G. Efficiency of catalytic processes for the reduction of CO and VOC emissions from wood combustion in domestic fireplaces. *Fuel Process. Technol.* **2009**, *90*, 1053–1061. [[CrossRef](#)]
18. Kaivosoja, T.; Virén, A.; Tissari, J.; Ruuskanen, J.; Tarhanen, J.; Sippula, O.; Jokiniemi, J. Effects of a catalytic converter on PCDD/F, chlorophenol and PAH emissions in residential wood combustion. *Chemosphere* **2012**, *88*, 278–285. [[CrossRef](#)]
19. Corro, G.; Pal, U.; Ayala, E.; Vidal, E. Diesel soot oxidation over silver-loaded SiO₂ catalysts. *Catal. Today* **2013**, *212*, 63–69. [[CrossRef](#)]

20. Shimizu, K.; Kawachi, H.; Satsuma, A. Study of active sites and mechanism for soot oxidation by silver-loaded ceria catalyst. *Appl. Catal. B Environ.* **2010**, *96*, 169–175. [[CrossRef](#)]
21. Nossova, L.; Caravaggio, G.; Couillard, M.; Ntais, S. Effect of preparation method on the performance of silver-zirconia catalysts for soot oxidation in diesel engine exhaust. *Appl. Catal. B Environ.* **2018**, *225*, 538–549. [[CrossRef](#)]
22. Aneggi, E.; Llorca, J.; de Leitenburg, C.; Dolcetti, G.; Trovarelli, A. Soot combustion over silver-supported catalysts. *Appl. Catal. B Environ.* **2009**, *91*, 489–498. [[CrossRef](#)]
23. Yamazaki, K.; Kayama, T.; Dong, F.; Shinjoh, H. A mechanistic study on soot oxidation over CeO₂-Ag catalyst with ‘rice-ball’ morphology. *J. Catal.* **2011**, *282*, 289–298. [[CrossRef](#)]
24. Castro, A.; Calvo, A.I.; Blanco-Alegre, C.; Oduber, F.; Alves, C.; Coz, E.; Amato, F.; Querol, X.; Fraile, R. Impact of the wood combustion in an open fireplace on the air quality of a living room: Estimation of the respirable fraction. *Sci. Total Environ.* **2018**, *628–629*, 169–176. [[CrossRef](#)]
25. Shromova, O.A.; Kinnunen, N.M.; Pakkanen, T.A.; Suvanto, M. Promotion effect of water in catalytic fireplace soot oxidation over silver and platinum. *RSC Adv.* **2017**, *7*, 46051–46059. [[CrossRef](#)]
26. Liu, S.; Wu, X.; Weng, D.; Ran, R. Ceria-based catalysts for soot oxidation: A review. *J. Rare Earths* **2015**, *33*, 567–590. [[CrossRef](#)]
27. Moreno-Castilla, C.; Pérez-Cadenas, A.; Moreno-Castilla, C.; Pérez-Cadenas, A.F. Carbon-Based Honeycomb Monoliths for Environmental Gas-Phase Applications. *Materials* **2010**, *3*, 1203–1227. [[CrossRef](#)]
28. Gatica, J.M.; Rodríguez-Izquierdo, J.M.; Sánchez, D.; Ania, C.; Parra, J.B.; Vidai, H. Extension of preparation methods employed with ceramic materials to carbon honeycomb monoliths. *Carbon* **2004**, *42*, 3251–3254. [[CrossRef](#)]
29. Ridha, F.N.; Manovic, V.; Macchi, A.; Anthony, E.J. The effect of SO₂ on CO₂ capture by CaO-based pellets prepared with a kaolin derived Al(OH)₃ binder. *Appl. Energy* **2012**, *92*, 415–420. [[CrossRef](#)]
30. Medri, V.; Fabbri, S.; Ruffini, A.; Dedeczek, J.; Vaccari, A. SiC-based refractory paints prepared with alkali aluminosilicate binders. *J. Eur. Ceram. Soc.* **2011**, *31*, 2155–2165. [[CrossRef](#)]
31. Kim, E.-H.; Lee, J.-H.; Jung, Y.-G.; Jang, J.-C.; Paik, U. Control of H₂O generated during the CO₂ hardening process in a casting mold. *Ceram. Int.* **2013**, *39*, 3993–3998. [[CrossRef](#)]
32. Luz, A.P.; Gomes, D.T.; Pandolfelli, V.C. High-alumina phosphate-bonded refractory castables: Al(OH)₃ sources and their effects. *Ceram. Int.* **2015**, *41*, 9041–9050. [[CrossRef](#)]
33. Vippola, M.; Keränen, J.; Zou, X.; Hovmöller, S.; Lepistö, T.; Mäntylä, T. Structural Characterization of Aluminum Phosphate Binder. *J. Am. Ceram. Soc.* **2004**, *83*, 1834–1836. [[CrossRef](#)]
34. Chung, D.D.L.L. Review: Acid aluminum phosphate for the binding and coating of materials. *J. Mater. Sci.* **2003**, *38*, 2785–2791. [[CrossRef](#)]
35. Leofanti, G.; Padovan, M.; Tozzola, G.; Venturelli, B. Surface area and pore texture of catalysts. *Catal. Today* **1998**, *41*, 207–219. [[CrossRef](#)]
36. Richardson, J.T. *Principles of Catalyst Development*, 1st ed.; Plenum Press: New York, NY, USA, 1989; p. 28.
37. Hagen, J. *Industrial Catalysis a Practical Approach*, 3rd ed.; John Wiley & Sons: Hoboken, NJ, USA, 2015; p. 179.
38. Richardson, J.T. *Principles of Catalyst Development*, 1st ed.; Plenum Press: New York, NY, USA, 1989; p. 162.
39. Gardini, D.; Christensen, J.M.; Damsgaard, C.D.; Jensen, A.D.; Wagner, J.B. Visualizing the mobility of silver during catalytic soot oxidation. *Appl. Catal. B Environ.* **2016**, *183*, 28–36. [[CrossRef](#)]
40. Souza, A.D.V.; Arruda, C.C.; Fernandes, L.; Antunes, M.L.P.; Kiyohara, P.K.; Salomão, R. Characterization of aluminum hydroxide (Al(OH)₃) for use as a porogenic agent in castable ceramics. *J. Eur. Ceram. Soc.* **2015**, *35*, 803–812. [[CrossRef](#)]
41. Neeft, J.P.A.; Makkee, M.; Moulijn, J.A. Metal oxides as catalysts for the oxidation of soot. *Chem. Eng. J. Biochem. Eng. J.* **1996**, *64*, 295–302. [[CrossRef](#)]
42. Sadezky, A.; Muckenhuber, H.; Grothe, H.; Niessner, R.; Pöschl, U. Raman microspectroscopy of soot and related carbonaceous materials: Spectral analysis and structural information. *Carbon* **2005**, *43*, 1731–1742. [[CrossRef](#)]
43. Haneda, M.; Watanabe, T.; Kamiuchi, N.; Ozawa, M. Effect of platinum dispersion on the catalytic activity of Pt/Al₂O₃ for the oxidation of carbon monoxide and propene. *Appl. Catal. B Environ.* **2013**, *142*, 8–14. [[CrossRef](#)]

44. Hoost, T.E.; Kudla, R.J.; Collins, K.M.; Chattha, M.S. Characterization of Ag/ γ -Al₂O₃ catalysts and their lean-NO_x properties. *Appl. Catal. B Environ.* **1997**, *13*, 59–67. [[CrossRef](#)]
45. Neeft, J.P.A.; Makkee, M.; Moulijn, J.A. Catalysts for the oxidation of soot from diesel exhaust gases. I. An exploratory study. *Appl. Catal. B Environ.* **1996**, *8*, 57–78. [[CrossRef](#)]



© 2019 by the authors. Licensee MDPI, Basel, Switzerland. This article is an open access article distributed under the terms and conditions of the Creative Commons Attribution (CC BY) license (<http://creativecommons.org/licenses/by/4.0/>).